International Journal of Basic and Applied Sciences, 15 (2) (2026) 121-139

International Journal of Basic and Applied Sciences

Website: www.sciencepubco.com/index.php/IJBAS
https://doi.org/10.14419/m918a861
Research paper

Optimal Trajectories for The Control of A Truck-Type Mobile Robot Navigating A Roundabout

Vincent Kangbe [1*], Ouazna Oukacha [2], Adama Coulibaly [1]

[1] Université Félix Houphouet Boigny, Abidjan, Côte d'Ivoire
[2] ECAM Louis de Broglie, Rennes, France
**Corresponding author E-mail: kangbevincent@gmail.com*

Received: 21-02-2026, Accepted: 25-04-2026, Published: 21-08-2026

Abstract

This study investigates the optimal control of an autonomous truck-type system navigating circular obstacles, considering two performance criteria: minimizing travel time and minimizing energy consumption (control effort). The theoretical analysis employs the Pontryagin Maximum Principle (PMP), which provides necessary conditions for optimality by characterizing switching functions. Based on these conditions, optimal trajectories and corresponding control laws are derived.
Three case studies are presented: Time-Optimal Control of a Truck in the Absence of Circular Obstacles (TOCTACO), Time-Optimal Control of a Truck in the Presence of a Circular Obstacle (TOCTPCO), and Energy-Efficient Truck Path Planning in the Presence of Circular Obstacles (EETPPPCO). The obstacle-free case demonstrates that time-optimal controls follow a typical bang-bang structure. Introducing a circular obstacle modifies the control structure while preserving, under certain conditions, the bang-bang behavior for time minimization. For the energy-optimization scenario, PMP analysis shows that optimal controls may include singular arcs, whose presence and duration influence the trajectory smoothness, maneuver duration, and total energy consumption.
Numerical simulations, performed using a direct trapezoidal collocation method, model the obstacle as a roundabout, a traffic feature commonly encountered by trucks. The results confirm the theoretical predictions and demonstrate that the presence of singular arcs can reduce energy consumption compared to purely bang-bang strategies, even when the maneuver duration increases. The simulations also highlight the sensitivity of optimal trajectories to entry and exit configurations around the roundabout. These findings provide practical insights into the influence of environmental constraints on trajectory planning and support the development of energy-efficient and safe navigation strategies for autonomous truck systems. Future work will focus on designing an autonomous roundabout management strategy that accounts for truck dimensions and operational constraints.

Keywords: *Circular Obstacle; Energy Optimization; Mobile Robot; Optimal Control Theory; Pontryagin's Maximum Principle; Trajectory Planning.*

1. Introduction

Autonomous systems, particularly automotive-type mobile robots, are increasingly employed in fields such as autonomous driving, industrial logistics, and robotic exploration. Optimizing trajectories between two configurations remains a major challenge, as vehicles must comply with dynamic movement constraints while achieving performance objectives, such as minimizing travel time and energy consumption.
Navigating around circular obstacles, such as roundabouts, is a critical aspect of planning the movements of autonomous vehicles in complex urban environments. Optimizing the trajectories of truck-type robots under these conditions is not only a matter of performance but also essential for ensuring safety, maintaining efficient traffic flow, and complying with traffic regulations. The efficiency of a vehicle's trajectory around circular obstacles depends on both the control strategy and the vehicle's geometric characteristics, particularly the wheelbase length. The issues addressed in this study- trajectory planning under kinematic constraints, operating within constrained environments, and balancing speed with energy efficiency are directly relevant to scenarios inspired by real urban traffic. Beyond its theoretical interest, this study has practical applications in autonomous driving systems and mobile robotics.

1.1. State of the art

Trajectory planning and optimal control for mobile robots and autonomous vehicles have been extensively studied. The main objectives typically include minimizing travel time and energy consumption while ensuring safety and satisfying both dynamic and geometric constraints. For car-type vehicles and connected autonomous vehicles (CAVs), notable contributions include:

- Zhao et al. [46]: decentralized optimal control for mixed-traffic roundabouts, minimizing travel time and energy while ensuring safe coordination.

- Long et al. [30]: cooperative optimization emphasizing vehicle-to-vehicle interactions for smoother and more efficient trajectories.
- Xu, Cassandras, and Xiao [44]: decentralized time- and energy-optimal control for roundabouts, improving safety, comfort, and traffic efficiency.
- Chalaki and Beaver [12]: experimental validation of PMP-based controllers for multi-lane roundabouts, demonstrating practical feasibility.
- Farkas et al. [25]: MPC-based approaches for real-time trajectory planning in roundabouts.
- Beaver [18]: long-duration autonomy strategies for CAVs, ensuring robust and energy-efficient performance over extended operations.

For truck-type vehicles or wheeled robots with trailers, which introduce additional challenges such as nonholonomic constraints, articulated kinematics, and larger geometric dimensions, research includes:

- Rizano et al. [35]: global trajectory planning for competitive robotic cars.
- Bouzar Essaidi and Haddad [20]: minimum-time trajectory planning under dynamic constraints for wheeled robots with trailers.
- Zhao et al. [45]: trajectory planning and tracking for mobile tractor-trailer robots under multiple constraints.
- Babaei Robat et al. [15]: dynamic modeling and trajectory tracking for semi-trailer robots accounting for wheel slip.
- Shojaei [36]: intelligent and coordinated control of an autonomous semi-trailer and combine harvester.
- Chuan et al. [32]: energy-optimal trajectory planning for electric vehicles using inverse dynamics and servo constraints.
- Bouzar Essaidi et al. [19]: path planning for autonomous wheeled robots with trailers.

The present work adopts an optimal control framework where the vehicle dynamics are modeled as a classical nonholonomic system [24]. Unlike [33], this study considers an energy-cost function that explicitly incorporates both linear and angular velocities. The roundabout is modeled as a circular obstacle represented via a state constraint.

The complex interactions between vehicle dynamics, geometric limitations, and environmental constraints motivate this study, which aims to characterize the optimal control laws and switching functions that enhance safety, energy efficiency, and maneuverability.

1.2. Methodology

This study leverages Pontryagin's Maximum Principle (PMP) to analyze time- and energy-optimal control problems for a truck navigating a roundabout. PMP provides necessary conditions for optimality through a system of coupled differential equations derived from the Hamiltonian formulation. A key focus is the analysis of switching functions, which determine the instances at which longitudinal velocity and steering angle change regimes. These functions are crucial for understanding the structure of optimal trajectories in systems with bounded controls and nonholonomic constraints.

The optimal solution is computed using the direct trapezoidal collocation method, implemented in MATLAB [16]. Unlike indirect shooting methods, collocation efficiently solves large-scale problems involving state and control constraints. The proposed methodology comprises the following stages:

1) System modeling: Modeling of truck-type robot dynamics subject to nonholonomic constraints and characterized by geometric parameters (wheelbase, articulation).
2) Optimal control formulation: Formulation of optimal control problems aimed at minimizing travel time and energy consumption (control effort).
3) Analysis via PMP: Derivation of switching functions from the Hamiltonian to characterize optimal controls and determine switching conditions.
4) Numerical implementation: Solution of the optimal control problem using a collocation-based approach with explicit state and control constraints.
5) Simulation and evaluation: Evaluation of the influence of circular obstacles and vehicle geometry on trajectory evolution, control signals, energy consumption, and maneuverability.

1.3. Motivation and objectives

Truck-type autonomous systems face unique challenges arising from their nonholonomic dynamics, large size, and complex interactions with environmental obstacles. Efficient navigation requires strategies that are simultaneously energy-efficient, safe, and dynamically feasible. The main objectives of this study are to:

- Formulate and solve optimal control problems under time and energy criteria.
- Analyze system dynamics and PMP-related properties relevant to optimal control.
- Derive optimal control laws and switching functions for circular obstacle avoidance.
- Perform numerical simulations to evaluate the impact of obstacles and vehicle geometry on trajectory evolution, state dynamics, and energy consumption.
- Provide insights to enhance maneuverability and energy efficiency in truck-type autonomous systems operating in constrained environments.

This manuscript is a research article. Although a summary of existing work is included in the introduction to situate the study within the current scientific context, the main objective is to propose original mathematical formulations, establish their theoretical optimality conditions, and illustrate the results with numerical simulations applied to a nonholonomic mobile robot. This study also enables visualization of optimal trajectories for autonomous truck systems navigating roundabouts, while accounting for the complexity of intersections. The results aim to extend safe, energy-efficient, and robust control strategies to heavy autonomous vehicles operating in urban and multi-agent traffic scenarios.

The remainder of this paper is organized as follows. Section 2 introduces the truck-type mobile robot system and a circular obstacle in the plane. Section 3 addresses two time-minimization control problems: Time-Optimal Control of a Truck in the Absence of Circular Obstacles (TOCTACO) and Time-Optimal Control of a Truck in the Presence of a Circular Obstacle (TOCTPCO), including their analysis via Pontryagin's Maximum Principle (PMP). Section 4 presents the formulation of the truck control problem in the presence of a circular obstacle under an energy-minimization criterion (Energy-Efficient Truck Path Planning in the Presence of Circular Obstacles (EETPPPCO)), along with the determination of optimal controls using PMP. Numerical results and their discussion are presented in Section 5. Finally, Section 7 concludes the paper and outlines directions for future research.

2. Modeling of a Truck-Type Mobile Robot and a Circular Obstacle

Accurate modeling is a fundamental step in the analysis and control of mobile robotic systems. Truck-type mobile robots exhibit nonholonomic constraints and more complex kinematic behavior compared to simpler wheeled robots. In addition, the presence of obstacles in the environment introduces safety constraints that must be considered during motion planning. This section presents the kinematic modeling of a truck-type mobile robot and the geometric representation of a circular obstacle. The objective is to establish a mathematical framework that will be used for trajectory planning and collision avoidance.

2.1. Dynamic model of the truck

Consider a dynamic system of the truck type, as described in [42], with state vector $X = (x(t), y(t), \theta(t), \emptyset(t))^T \in \mathbb{R}^4$ and control vector $U = (u_1(t), u_2(t))^T \in \mathcal{U} \subset \mathbb{R}^2$. Here, X^T denotes the transpose of the vector X.

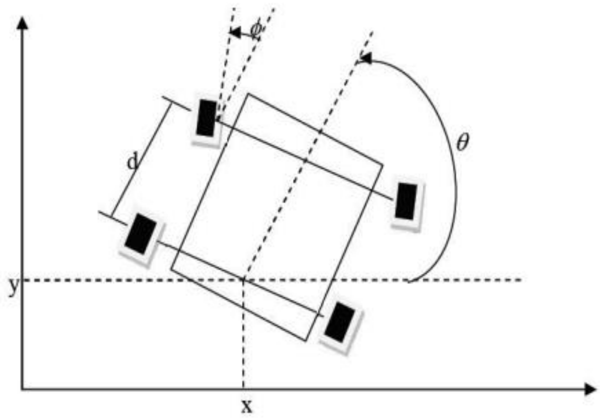

Fig. 1: Geometric Model of A Truck-Type Mobile Robot.

In the following, to simplify the notation, the time dependence of time-varying functions is omitted whenever it does not lead to ambiguity. The dynamics of a truck-type mobile robot, as illustrated in Figure 1, are described by the differential system (1).

$$\begin{cases} \dot{x} = u_1 \cos(\theta) \\ \dot{y} = u_1 \sin(\theta) \\ \dot{\theta} = u_1 \frac{tan(\phi)}{d} \\ \dot{\phi} = u_2 \end{cases}$$

with $\theta = \arctan\left(\frac{\dot{y}}{\dot{x}}\right)$ and $|u_1| = \sqrt{\dot{x}^2 + \dot{y}^2}$. (1)

Where

- (x, y) denotes the position of the robot in Cartesian coordinates at time t in the fixed reference frame (O, X, Y).
- θ denotes the orientation (heading angle) of the truck with respect to the X-axis.
- $\emptyset$ denotes the steering angle (turning angle) of the truck's front wheels.
- d denotes the distance between the front and rear axles of the truck (the wheelbase).
- u_1 denotes the longitudinal velocity of the truck.
- u_2 denotes the angular velocity of the steering wheels relative to the truck body.
- $U = (u_1, u_2)^T$ denotes the control input vector.

The kinematic model of a nonholonomic truck-type mobile robot is obtained by applying transformations to the rolling constraints without lateral slip, as follows:

$$\dot{x}\sin(\theta) - \dot{y}\cos(\theta) = 0$$
$$\dot{x}\sin(\theta + \phi) - \dot{y}\cos(\theta + \phi) - d\cos\phi\dot{\theta} = 0 \quad (2)$$

These constraints are non-integrable, rendering the vehicle nonholonomic.

2.2. Obstacle avoidance constraint for a circular obstacle

A fixed circular obstacle is represented in the fixed reference frame (O, X, Y) as illustrated in Figure 2.

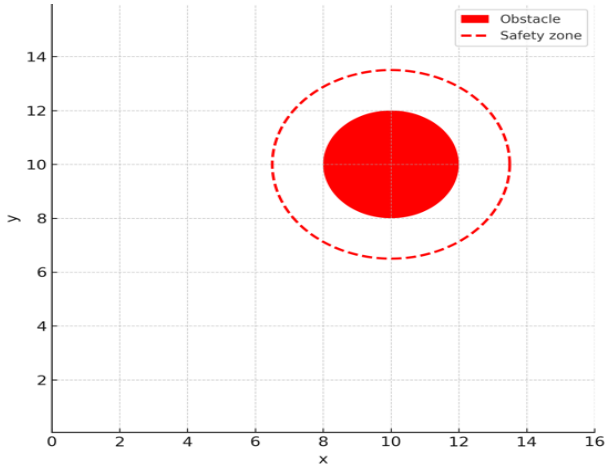

Fig. 2: Circular Obstacle with Safety Distance Used for Collision Avoidance.

The scenario of circular obstacle avoidance for a truck-type mobile robot is described by the following equation:

$$\sqrt{(x - x_{obs})^2 + (y - y_{obs})^2} \geq R \tag{3}$$

Where R is the radius of the restricted area, and (x_{obs}, y_{obs}) denotes the center of the obstacle. In general, $R = r_{obs} + d_s$, with r_{obs}being the radius of the obstacle and d_s being the safety distance.

3. Time-Optimal Control of a Truck via PMP

This section investigates the time-optimal control problem for a truck-type mobile robot. The objective is to drive the vehicle from an initial configuration to a desired final configuration in minimum time while satisfying its kinematic constraints. Both cases are considered: motion in free space and navigation in the presence of a circular obstacle, where collision-avoidance constraints influence the structure of the optimal control.

3.1. Time-optimal controlofa truckin the presence of a circular obstacle (TOCTPCO)

The problem of determining the optimal control for a truck-type mobile robot navigating in an environment containing a circular obstacle, under a time-minimization criterion, can be formulated as follows:

$$(TOCTPCO) = \begin{cases} \text{Minimize} \qquad J = \int_0^{T_f} dt \\ \text{Subject to} \\ \qquad \dot{x} = u_1 \cos(\theta) \\ \qquad \dot{y} = u_1 \sin(\theta) \\ \qquad \dot{\theta} = u_1 \frac{tan(\phi)}{d} \\ \qquad \dot{\phi} = u_2 \\ \qquad R - \sqrt{(x - x_{obs})^2 + (y - y_{obs})^2} \leq 0 \\ \qquad |u_1| \leq u_1^{max} \\ \qquad |u_2| \leq u_2^{max} \\ \qquad T_f : free \end{cases} \tag{4}$$

3.2. Application of Pontryagin’s Maximum Principle (PMP)

This paper employs Pontryagin's Maximum Principle (PMP) [34] as the main analytical tool, as it provides the necessary conditions for optimality in optimal control problems. Pontryagin’s Maximum Principle (PMP) guarantees the existence of:

- An absolutely continuous function $P : [0, T_f] \to \mathbb{R}^4$, representing the adjoint vector.
- A Lagrange multiplier μ: $[0, T_f] \to \mathbb{R}$, associated with the obstacle state constraint.

The Lagrange multiplier μ is continuous along the boundary arc and satisfies the following complementarity condition:

$$\mu \left(R - \sqrt{(x(t) - x_{\text{obs}})^2 + (y(t) - y_{\text{obs}})^2} \right) = 0, \quad \forall t \in [0, T_f]$$

By introducing the adjoint vector $P = \left(p_x, p_y, p_\theta, p_\emptyset\right)^T$, corresponding to the state vector $X = (x, y, \theta, \emptyset)^T$, and considering the control vector $U = (u_1, u_2)^T \in \mathcal{U} = [-u_1^{max}, u_1^{max}] \times [-u_2^{max}, u_2^{max}] \subset \mathbb{R}^2$ representing the truck commands. Since the problem in (4) is autonomous, the Hamiltonian remains constant along extremal trajectories and is denoted by

$$H = -1 + \mu\left(R - \sqrt{(x(t)-x_{obs})^2 + (y(t)-y_{obs})^2}\right) + \left(p_x\cos(\theta) + p_y\sin(\theta) + p_\theta\frac{tan(\phi)}{d}\right)u_1 + p_\phi u_2 \tag{5}$$

- Transversality condition: If the final time T_f is not fixed (free), then the Hamiltonian $H = 0$ along the extremal trajectory.

According to the necessary conditions for optimality given by Pontryagin's Maximum Principle (PMP), the adjoint equations for this system are:

$$\begin{cases} \dot{p}_x &= -\frac{\partial H}{\partial x} = \frac{\mu(x-x_{obs})}{\sqrt{(x-x_{obs})^2+(y-y_{obs})^2}} \\ \dot{p}_y &= -\frac{\partial H}{\partial y} = \frac{\mu(y-y_{obs})}{\sqrt{(x-x_{obs})^2+(y-y_{obs})^2}} \\ \dot{p_\theta} &= -\frac{\partial H}{\partial \theta} = \big(p_x\sin(\theta) - p_y\cos(\theta)\big)u_1 \\ \dot{p_\phi} &= -\frac{\partial H}{\partial \phi} = -\frac{p_\theta u_1}{d}\left(1 + tan(\phi)^2\right) \end{cases} \tag{6}$$

In this case, the maximum of the Hamiltonian function is expressed as follows:

$$H(X,U^*,P) = -1 + \mu\left(R - \sqrt{(x(t)-x_{obs})^2 + (y(t)-y_{obs})^2}\right) + \max_{(u_1,u_2)\in\mathcal{U}}\{\psi_1(t)u_1 + \psi_2(t)u_2\} \tag{7}$$

Where ψ_1 and ψ_2 represent the switching functions, defined as:

$$\psi_1 = p_x\cos(\theta) + p_y\sin(\theta) + p_\theta\frac{\tan(\phi)}{d} \qquad \text{and} \qquad \psi_2 = p_\phi \tag{8}$$

In this case, the Hamiltonian is linear with respect to the controls. The switching functions simplify accordingly, and the optimal control $U^* = (u_1^*, u_2^*)^T$ meets the following conditions:

$$u_1^*\begin{cases} = u_1^{max} & if\ \ \psi_1 > 0 \\ = -u_1^{max} & if\ \ \psi_1 < 0 \\ \in]-u_1^{max}, u_1^{max}[& if\ \ \psi_1 = 0 \end{cases} \ and\ \ u_2^*\begin{cases} = u_2^{max} & if\ \ \psi_2 > 0 \\ = -u_2^{max} & if\ \ \psi_2 < 0 \\ \in]-u_2^{max}, u_2^{max}[& if\ \ \psi_2 = 0 \end{cases} \tag{9}$$

Remark 1: *Possible optimal solutions for optimization problem~(4) under the obstacle-avoidance condition are summarized as follows:*

- The Hamiltonian Boundary-Value Problem (HBVP) is defined by the state and costate dynamics $(\dot{X}, \dot{P})$ together with their initial and terminal conditions, namely $X(0), X(T), P(0)$ and $P(T)$.
- An extremal solution is a quadruple (X, P, p_0, U) satisfying the above equations. An extremal is said to be normal whenever $p_0 \neq 0$ and abnormal whenever $p_0 = 0$. The component p_0 corresponds to the Lagrange multiplier associated with the cost function. In the normal case $p_0 \neq 0$, it is common to normalize the Lagrange multiplier so that $p_0 = -1$. Finally, note the convention. $p_0 \leq 0$ in the PMP leads to a maximization condition of the Hamiltonian (the convention $p_0 \geq 0$ would lead to a minimization condition).
- A solution is said to be of bang-bang type if the control takes its extreme values, i.e., the maximum$(u_i = u_i^{max}, i = 1,2)$ or the minimum value $(u_i = -u_i^{max}, i = 1,2)$.

In this case, the switching function satisfies. $\psi_i(t) > 0$ for the maximum value and $\psi_i(t) < 0$ for the minimum value.

- A singular arc is defined as a portion of the extremal trajectory along which the control does not attain its extreme values (maximum or minimum). This situation occurs when the corresponding switching function satisfies $\psi_i(t) = 0$ over a nonzero time interval.
- An extremal trajectory with inactivation is defined when the control variable is equal to zero over a time interval.

However, the adjoint equation system (6) remains complex, and analyzing singular arcs is more involved in this context. For clarity, we first consider the minimum-time problem in the absence of obstacles.

3.3. Time-optimal control of a truck in the absence of circular obstacles (TOCTACO)

For the truck system in the absence of obstacles, the Hamiltonian simplifies to:

$$H(X,U,P) = -1 + \left(p_x\cos\theta + p_y\sin\theta + p_\theta\frac{\tan(\phi)}{d}\right)u_1 + p_\phi u_2. \tag{10}$$

The adjoint vectors are similar to those of system (6), except that. $\dot{p}_x = \dot{p}_y = 0$, in the absence of obstacles.
The maximization of the Hamiltonian is given by:

$$H(X,U^*,P) = -1 + \max_{(u_1,u_2)\in\mathcal{U}}\{\psi_1 u_1 + \psi_2 u_2\}, \tag{11}$$

Where ψ_1 and ψ_2 are defined as in Equation (8).

The switching functions ψ_1 and ψ_2 are simplified, as the adjoint equations are also simplified in the absence of obstacles. The optimal control is then given by $U^* = (u_1^*, u_2^*)^T$, where u_1^* and u_2^* are defined analogously to the system controls in (9).
Consequently, the optimal control $U^* = (u_1^*, u_2^*)^T$ can be classified into four distinct cases according to the signs and values of its components:

$$\begin{cases} \textbf{Case 1:} & u_1 = u_1^{cst}, \;\; u_1^{cst} = |u_1^{max}|, \;\; u_2 = u_2^{cst}, \;\; u_2^{cst} = |u_2^{max}| \\ \textbf{Case 2:} & u_1 = u_1^{cst}, \;\; u_2 \in]-u_2^{max}, u_2^{max}[, \;\; \psi_2 = 0 \\ \textbf{Case 3:} & u_1 \in]-u_1^{max}, u_1^{max}[, \;\; \psi_1 = 0, \;\; u_2 = u_2^{cst} \\ \textbf{Case 4:} & u_1 \in]-u_1^{max}, u_1^{max}[, \;\; \psi_1 = 0, \;\; u_2 \in]-u_2^{max}, u_2^{max}[, \;\; \psi_2 = 0 \end{cases} \tag{12}$$

The optimal solution to the minimum-time problem is determined by a combination of these four cases. The optimal control may be of bang-bang type, meaning that its components switch between the boundary values of the admissible control set, or of constant type, as in Case 1.
In Cases 2, 3, and 4, the control may be either constant or of mixed type. In Case 4, it may additionally vary continuously along the trajectory.

3.4. Theoretical analysis of singular arcs

In general, the most important aspect in the study of minimum-time problems concerns the analysis of singular arcs. This requires a more detailed examination of Cases 2, 3, and 4, as presented in Proposition (1)
Proposition1. Bang-bang control for problem (TOCTACO)
For a truck-type mobile robot moving without obstacles, the minimum-time optimal trajectory is achieved using bang-bang controls u_1 and u_2.
Proof.
The proof demonstrates that the minimum-time, obstacle-free problem does not admit any singular arcs. The analysis of singular controls focusing on their structure and behavior constitutes the core of the proof, which ultimately identifies the optimal trajectory as described in Cases 2, 3, and 4 (see Equation (12))

- Case 2: $u_1 = u_1^{Cst}$ and $u_2 \in]-u_2^{max}, u_2^{max}[$ with $\psi_2(t) = 0$

Since with $\psi_2 = p_\emptyset = 0$, it follows that $\dot{p}_\emptyset = 0$. From the adjoint equation (cf. Equation (6)) for $\dot{p}_\emptyset = 0$, we obtain $p_\theta = 0$, which implies

$$\dot{p}_\theta = (p_x \sin\theta - p_y \cos\theta) u_1 = 0$$

Since $u_1 \neq 0$, we obtain $p_x \sin\theta - p_y \cos\theta = 0$.

Since $\dot{p}_x = \dot{p}_y = 0$, which yields

$$\theta = \arctan\left(\frac{p_y}{p_x}\right) = \text{const},\ p_x \neq 0$$

From the kinematic equation of the truck, we have $\dot{\theta} = \frac{u_1}{d}\tan(\emptyset)$.
Since θ is constant, it follows that $\dot{\theta} = 0$. As $u_1 \neq 0$, we deduce $\tan(\emptyset) = 0$, then $\emptyset = 0$.
Differentiating $\dot{\theta}$, we obtain

$$\ddot{\theta} = \frac{u_1}{d}(1 + \tan^2\emptyset)\dot{\emptyset} = 0.$$

Therefore,

$$\dot{\emptyset} = u_2 = 0$$

In conclusion, $u_1 = \text{const}$ and $u_2 = 0$, and the robot follows a straight-line trajectory.

- Case 3: $u_1 \in]-u_1^{max}, u_1^{max}[$ with $\psi_1(t) = 0$ and $u_2 = u_2^{Cst}$

Since $\psi_1(t) = 0$, the Hamiltonian reduces to

$$H(t) = -1 + \psi_2 u_2^{Cst}$$

As the Hamiltonian is autonomous and the final time is free, we have $H(t) = 0$, which implies that ψ_2 is constant with $u_2^{Cst} \neq 0$. Consequently, $\dot{\psi}_2 = \dot{p}_\emptyset = 0$, and therefore $p_\theta = 0$.
Proceeding as in Case 2, we obtain $\theta = \text{const}$, which implies: $\dot{\theta} = 0$, $\tan(\emptyset) = 0$ and $u_2 = 0$.
This contradicts the assumption that $u_2 = u_2^{Cst} \neq 0$. In conclusion, Case 3 is not feasible.

- Case 4: $u_1 \in]-u_1^{max}, u_1^{max}[$ with $\psi_1(t) = 0$ and $u_2 \in]-u_2^{max}, u_2^{max}[$ with $\psi_2(t) = 0$

In this case, both switching functions vanish, and the Hamiltonian reduces to

$H(t) = -1, \forall t \in [0, T_f]$

However, since the Hamiltonian is autonomous and the final time T_f is free, the transversality condition requires that

$H(t) = 0.$

This leads to the contradiction. $H(t) = -1 \neq 0$.
Therefore, Case 4 is not feasible.
Conclusion: Therefore, the minimum-time problem without obstacles (TOCTWO) does not admit singular arcs. The optimal control is of bang-bang type.
In contrast to the minimum-time problem in the absence of obstacles (TOCTACO), the problem in the presence of obstacles (TOCTPCO) may admit singular arcs under certain conditions, as established in the following proposition (see Proposition 2).
Proposition 2. Singular Arc Control in Certain Cases for Problem (TOCTPCO)
The optimal trajectory of a truck-type mobile robot navigating around a circular obstacle under the minimum time criterion may involve a singular control arc in specific situations where the control direction varies while its norm remains constant.
Proof. The proof follows the same methodological approach as that outlined in Proposition 1. By analyzing the Hamiltonian system and the associated adjoint equations, we observe the following cases:

- Case 2: $u_1 = u_1^{Cst}$ and $u_2 \in]-u_2^{max}, u_2^{max}[$ with $\psi_2(t) = 0$

Similar to Case 2 of problem (TOCTWO), but with adjoint vectors p_x and p_y given by Equation (6):

$$\theta = \arctan\left(\frac{p_y}{p_x}\right), \quad p_x \neq 0 \tag{13}$$

Two scenarios arise:

If $p_x = p_y$: $\dot{\theta} = 0, \tan(\emptyset) = 0, \emptyset = n\pi, n \in \mathbb{Z}$.

Hence, $\dot{\emptyset} = u_2 = 0$, $U = (u_1^{Cst}, 0)$, with $u_1^{Cst} = \pm u_1^{max}$,

And the truck moves in a straight line without turning.

If $p_x \neq p_y$:

$$\phi = \arctan\left(\frac{d(\dot{p}_y p_x - \dot{p}_x p_y)}{u_1(p_x^2 + p_y^2)}\right), \quad u_2 = \dot{\phi},$$

Which leads to a complex singular arc. The system is singular in this scenario.

- Case 3: $u_1 \in]-u_1^{max}, u_1^{max}[$ with $\psi_1(t) = 0$ and $u_2 = u_2^{Cst}$

From Equation (8),

$$\psi_1 = p_x \cos\theta + p_y \sin\theta + p_\theta \frac{\tan\phi}{d} = 0.$$

The first derivative and

$$\dot{\theta} = \frac{u_1 \tan\phi}{d}, \quad \dot{p}_\theta = (p_x \sin\theta - p_y \cos\theta)u_1,$$

$$\dot{\psi}_1 = \dot{p}_x \cos\theta + \dot{p}_y \sin\theta + \frac{p_\theta}{d}(1 + \tan^2\phi)\dot{\phi} = 0.$$

Yield
The second derivative is

$$\ddot{\psi}_1 = \ddot{p}_x \cos\theta + \ddot{p}_y \sin\theta - (\dot{p}_x \sin\theta - \dot{p}_y \cos\theta)\dot{\theta} + \frac{\dot{p}_\theta}{d}(1 + \tan^2\phi)\dot{\phi}$$
$$+ \frac{p_\theta}{d}\left[(1 + \tan^2\phi)\ddot{\phi} + 2\tan\phi(1 + \tan^2\phi)\dot{\phi}^2\right].$$

Substituting from Equation (14) gives

$$\ddot{\psi}_1 = \ddot{p}_x \cos\theta + \ddot{p}_y \sin\theta - (\dot{p}_x \sin\theta - \dot{p}_y \cos\theta)\frac{u_1 \tan\phi}{d} + \frac{(p_x \sin\theta - p_y \cos\theta)u_1}{d}(1 + \tan^2\phi)\dot{\phi}$$
$$+ \frac{p_\theta}{d}\left[(1 + \tan^2\phi)\ddot{\phi} + 2\tan\phi(1 + \tan^2\phi)\dot{\phi}^2\right] = 0. \tag{15}$$

This equation implicitly defines a singular arc. Analytical determination of u1 is complex, and numerical methods are generally required.

- Case 4: $u_1 \in]-u_1^{max}, u_1^{max}[$ with $\psi_1(t) = 0$ and $u_2 \in]-u_2^{max}, u_2^{max}[$ with $\psi_2(t) = 0$

The Hamiltonian is

$$H = -1 + \mu\Big(R - \sqrt{(x - x_{\text{obs}})^2 + (y - y_{\text{obs}})^2}\Big).$$

Since $H(t) = H(T_f)$, we would require
By the complementarity condition, this is impossible:

$$\mu\Big(R - \sqrt{(x - x_{\text{obs}})^2 + (y - y_{\text{obs}})^2}\Big) = 1.$$

$$\mu\Big(R - \sqrt{(x - x_{\text{obs}})^2 + (y - y_{\text{obs}})^2}\Big) = 0.$$

Hence, Case 4 is impossible; no singular arcs exist, and the robot follows a straight-line trajectory.
Conclusion: Singular arcs in the time-optimal control problem with a circular obstacle (TOCTPCO) occur only in Case 2 when $p_x \neq p_y$, corresponding to a singular arc in the control u_2, and in Case 3, which involves a complex singular arc in the control u_1.
All other cases lead either to bang-bang controls or to straight-line motion. When present, singular arcs are complex and typically require numerical methods for their determination.
Unlike the obstacle-free problem (TOCTACO), which does not admit singular arcs (cf. Proof of Proposition 1), the problem with obstacles (TOCTPCO) may admit singular arcs under certain conditions (cf. Proof of Proposition 2).
The final problem we study theoretically is an energy-optimal problem, where the cost function penalizes the system's energy rather than travel time. This formulation evaluates how the presence of a circular obstacle influences the occurrence and structure of singular arcs for a truck-type mobile robot.

4. Energy-Efficient Truck Path Planning in The Presence of Circular Obstacles (EETPPPCO)

This section addresses the problem of planning energy-efficient paths for a truck-type mobile robot navigating in environments with circular obstacles. The goal is to minimize the total energy consumption while satisfying the vehicle's kinematic constraints and avoiding collisions. Both constant and variable control strategies are analyzed to determine optimal energy trajectories.

4.1. Modeling for the problem (EETPPPCO)

For a truck-type mobile robot, a common approach to energy-efficient path planning is to penalize both linear and angular velocities. This helps minimize energy consumption while ensuring smooth speed regulation and maneuverability. A quadratic cost function is typically used, as squaring the control terms guarantees non-negative contributions and leads to smoother optimization. Accordingly, the control effort (energy cost) of the truck is modeled by the following equation:

$$J = \frac{1}{2}\int_0^{T_f} (u_1^2 + u_2^2)dt \tag{16}$$

Accordingly, the energy-optimal control problem for a truck-type mobile robot navigating around a circular obstacle can be formulated as:

$$(EETPPPCO) = \begin{cases} \text{Minimize} \qquad J = \frac{1}{2}\int_0^{T_f} (u_1^2 + u_2^2)dt \\ \text{Subject to} \\ \qquad \dot{x} = u_1\cos(\theta) \\ \qquad \dot{y} = u_1\sin(\theta) \\ \qquad \dot{\theta} = u_1\frac{tan(\phi)}{d} \\ \qquad \dot{\phi} = u_2 \\ \qquad R - \sqrt{(x - x_{obs})^2 + (y - y_{obs})^2} \leq 0 \\ \qquad |u_1| \leq u_1^{max} \\ \qquad |u_2| \leq u_2^{max} \\ \qquad T_f : fixed \end{cases} \tag{17}$$

4.2. Singular arc analysis for the problem (EETPPPCO) via PMP

The Hamiltonian for the energy-optimal control problem (EETPPPCO) is defined as:

$$H = -\frac{1}{2}(u_1^2 + u_2^2) + \mu\left(R - \sqrt{(x - x_{obs})^2 + (y - y_{obs})^2}\right) + \left(p_x\cos\theta + p_y\sin\theta + p_\theta\frac{\tan\phi}{d}\right)u_1 + p_\phi u_2. \tag{18}$$

Since the problem (EETPPPCO) is autonomous, the Hamiltonian is constant along optimal trajectories; however, $H \neq 0$ because the final time is fixed.
The adjoint equations are identical to those of system (6).
The optimal control is then obtained by maximizing the Hamiltonian with respect to (u_1, u_2):

$$H(X,U^*,P) = \mu\left(R - \sqrt{(x-x_{obs})^2 + (y-y_{obs})^2}\right) + \max_{(u_1,u_2)\in\mathcal{U}} \{\psi_1(t) + \psi_2(t)\} \tag{19}$$

With

$$\begin{cases} \psi_1 & = -\frac{1}{2}u_1^2 + \left(p_x \cos(\theta) + p_y \sin(\theta) + p_\theta \frac{tan(\phi)}{d}\right) u_1 \\ \psi_2 & = -\frac{1}{2}u_2^2 + p_\phi u_2 \end{cases} \tag{20}$$

According to Pontryagin's Maximum Principle (PMP), the optimal control $U^* \in \arg\max_{U\in\mathcal{U}} H(X,U,P)$
Thus, the optimal control strategy is determined by $\max_{U\in\mathcal{U}} H(X,U,P)$, which relies on the switching function ψ_i for $i = 1,2$ as defined in Equation (20).
Here, the Hamiltonian function is quadratic with respect to the control variables. Within the admissible control set, the optimal controls correspond to the maximizers of the switching functions. These controls are determined by the stationary points of the switching functions, obtained by setting the first derivatives equal to zero:
Since the sufficient second-order condition given in Equation (22) is satisfied, the stationary points correspond to maxima of the Hamiltonian, and therefore the resulting controls are optimal.

$$\frac{\partial \psi_1}{\partial u_1} = 0 \quad \text{and} \quad \frac{\partial \psi_2}{\partial u_2} = 0 \tag{21}$$

$$\begin{cases} \dfrac{\partial^2 \psi_1}{\partial u_1^2} & = -1 < 0, \\ \dfrac{\partial^2 \psi_2}{\partial u_2^2} & = -1 < 0 \end{cases} \tag{22}$$

The optimal controls, corresponding to the absolute maxima of the switching functions $\psi_1(t)$ and $\psi_2(t)$, are given by the following control inputs:

$$\tilde{u}_1(t) = p_x \cos(\theta) + p_y \sin(\theta) + p_\theta \frac{\tan(\phi)}{d} \quad \text{and} \quad \tilde{u}_2(t) = p_\phi \tag{23}$$

The optimal controls depend on the signs of the system's adjoint variables (see Equation (6)). Thus, the final optimal controls u_1^* and u_2^* are obtained by applying the orthogonal projection operator to the unconstrained expressions $\tilde{u}_1(t)$ and $\tilde{u}_2(t)$. This ensures that both the optimality conditions of Pontryagin's Maximum Principle and the control constraints are satisfied simultaneously. The result is:

$$u_1^*(t) = \Pi_{[-u_1^{\max},\, u_1^{\max}]}(\tilde{u}_1(t)), \qquad u_2^*(t) = \Pi_{[-u_2^{\max},\, u_2^{\max}]}(\tilde{u}_2(t)) \tag{24}$$

Where $\tilde{u}_1(t)$ and $\tilde{u}_2(t)$ denote the unconstrained optimal controls defined in Equation (23), and where $\Pi_{\mathcal{U}}$ represents the projection operator onto the admissible control set $\mathcal{U}$.

$$\Pi_{\mathcal{U}} : \mathbb{R}^m \to \mathcal{U}$$

$$\Pi_{\mathcal{U}}(v) = \arg\min_{u\in\mathcal{U}} \|u - v\|, \qquad \forall v \in \mathbb{R}^m.$$

We define the projection operator Such that
Consequently, the optimal admissible controls can be written as

$$\begin{cases} u_1^*(t) = \begin{cases} -u_1^{\max}, & \text{if } \bar{u}_1(t) \le -u_1^{\max}, \\ \bar{u}_1(t), & \text{if } -u_1^{\max} < \bar{u}_1(t) < u_1^{\max}, \\ u_1^{\max}, & \text{if } \bar{u}_1(t) \ge u_1^{\max}, \end{cases} \\ \\ u_2^*(t) = \begin{cases} -u_2^{\max}, & \text{if } \bar{u}_2(t) \le -u_2^{\max}, \\ \bar{u}_2(t), & \text{if } -u_2^{\max} < \bar{u}_2(t) < u_2^{\max}, \\ u_2^{\max}, & \text{if } \bar{u}_2(t) \ge u_2^{\max}. \end{cases} \end{cases} \quad (25)$$

Proposition 3. Constant Controls Subject to Phase Constraints
Assuming that the Lagrange multiplier μ remains constant, the optimal trajectories of the truck-type mobile robot system, under an energy minimization criterion, correspond to constant control inputs u_1 and u_2 over the corresponding phase interval.
Proof. The proof relies on the autonomous nature of the system, which implies that the Hamiltonian. H remains constant along any extremal trajectory. Furthermore, it is assumed that the Lagrange multiplier. μ is constant. In this context, singular arcs are defined by the switching functions. $\psi_1(t) = 0$ and $\psi_2(t) = 0$.
Based on equation (20), the switching functions satisfy the following conditions:

- If $\psi_1(t) = 0$, then

$$\left(-\frac{u_1}{2} + \left(p_x \cos\theta + p_y \sin\theta + p_\theta \frac{\tan\phi}{d}\right)\right) u_1 = 0$$

Since $u_1 \neq 1$ (as $u_1 = 0$ corresponds to zero linear velocity of the vehicle, implying no displacement), it follows that $u_1 = 2\left(p_x \cos\theta + p_x \sin\theta + p_\theta \frac{\tan\emptyset}{d}\right)$

- If $\psi_1(t) = 0$, then $\left(-\frac{u_2}{2} + p_\emptyset\right) u_2 = 0$,

Which yields $u_2 = 0$ or $u_2 = 2p_\emptyset$
According to the possible values of u_1 and u_2, several combinations of singular arcs can be distinguished.

1) Condition 1: $u_1 = 2\left(p_x \cos\theta + p_x \sin\theta + p_\theta \frac{\tan\emptyset}{d}\right)$ and $u_2 = 0$

Under this condition, the Hamiltonian reduces to the expression associated with the obstacle constraint:

$$H(t) = \mu\left(R - \sqrt{(x(t) - x_{obs})^2 + (y(t) - y_{obs})^2}\right)$$

Since the Hamiltonian is constant along extremal trajectories and using the adjoint equations (6), we have:

$$\begin{aligned} \frac{dH}{dt} &= 0, \\ \dot{p}_x \dot{x} + \dot{p}_y \dot{y} &= 0, \\ (\dot{p}_x \cos\theta + \dot{p}_y \sin\theta) u_1 &= 0. \end{aligned} \quad (26)$$

Moreover, since $u_2 = \dot{\emptyset} = 0$, $\dot{\theta} = u_1 \frac{\tan\emptyset}{d}$ and $\dot{p}_\theta = (p_x \sin\theta - p_y \cos\theta) u_1$
The derivative of the control u1 simplifies to

$$\dot{u}_1 = 2(\dot{p}_x \cos\theta + \dot{p}_y \sin\theta).$$

Using equation (26) and the fact that $u_1 \neq 0$, we deduce: ˙ $\dot{u}_1$, and therefore

$$u_1 = \text{const}, u_2 = 0.$$

Hence, both control inputs remain constant along the singular arc.

2) Condition 2: $u_1 = 2\left(p_x \cos\theta + p_x \sin\theta + p_\theta \frac{\tan\emptyset}{d}\right)$ and $u_2 = 2p_\emptyset$

Similar to Condition 1, the derivative of the Hamiltonian allows us to obtain an equation similar to Equation 26, but the derivative of u_1 is given by

$$\dot{u}_1 = 2(\dot{p}_x \cos\theta + \dot{p}_y \sin\theta + p_\theta \frac{1 + \tan^2\emptyset)}{d} \dot{\emptyset})$$

Replace the latter in equation (26):

$$\dot{u}_1 u_1 = -\dot{u}_2 u_2$$

Integrating this relation gives $u_1^2(t) + u_2^2(t) = C$,
Where $C > 0$ is a constant.

Thus, the control effort remains constant along the trajectory.
The performance index becomes

$$J = \frac{1}{2}\int_0^{T_f} (u_1^2 + u_2^2)\, dt = \frac{1}{2}CT_f.$$

By polar parametrization $u_1 = C_0 \cos\psi(t), u_2 = C_0 \sin\psi(t)$ with $C_0 = \sqrt{C}$ and $\psi(t)$ the phase of (u_1, u_2). Controls are constant if and only if the phase $\psi(t)$ is constant; otherwise, the vehicle uses variable or mixed control, but with constant total energy.
In conclusion, under $u_1^2(t) + u_2^2(t) = C$, the vehicle travels along an optimal trajectory with constant total control effort, while individual controls may vary only in phase.

3) Condition 3: $u_1 = 2\left(p_x \cos\theta + p_x \sin\theta + p_\theta \frac{\tan\emptyset}{d}\right)$ and $u_2 = u_2^{Cst}$

Under this condition, the Hamiltonian becomes:

$$H(X,P,U) = -\frac{1}{2}(u_2^{Cst})^2 + p_\phi u_2^{Cst} + \mu(R - \sqrt{(x - x_{obs})^2 + (y - y_{obs})^2})$$

Since the Hamiltonian is constant, its time derivative satisfies $\frac{dH}{dt} = 0$, then

$$u_2^{Cst}\dot{p}_\phi - \dot{p}_x\dot{x} - \dot{p}_y\dot{y} = 0$$

$$\dot{\phi}\Big(- \frac{p_\theta u_1}{d}\left(1 + tan(\phi)^2\right) \Big) - \dot{p}_x\dot{x} - \dot{p}_y\dot{y} = 0$$

$$\left(\left(\frac{p_\theta}{d}\left(1 + tan(\phi)^2\right)\right)\dot{\phi} + \dot{p}_x\cos(\theta) + \dot{p}_y\sin(\theta)\right)u_1 = 0 \tag{27}$$

The first derivative of u_1, together with the expressions $\dot{\theta} = u_1 \frac{\tan\emptyset}{d}$ and $\dot{p}_\theta = (p_x \sin\theta - p_y \cos\theta)u_1$, allows us to deduce:

$$\dot{u}_1 = 2\Big(\dot{p}_x\cos(\theta) + \dot{p}_y\sin(\theta) + \left(\frac{p_\theta}{d}\left(1 + tan(\phi)^2\right)\right)\dot{\phi}\Big)$$

According to this last equation, equation (27) becomes: $\dot{u}_1 u_1 = 0$
Since $u_1 \neq 0$, it follows that $u_1 = \text{const}$, $u_2 = u_2^{cst}$.
Thus, both control inputs are constant.

4) Condition 4: $u_1 = u_1^{Cst}$ and $u_2 = 2p_\emptyset$

Consequently, the Hamiltonian takes the following form:

$$H = -\frac{1}{2}(u_1^{Cst})^2 + \left(p_x\cos(\theta) + p_y\sin(\theta) + p_\theta\frac{tan(\phi)}{d}\right)u_1^{Cst} + \mu\left(R - \sqrt{(x(t) - x_{obs})^2 + (y(t) - y_{obs})^2}\right)$$

As the Hamiltonian remains constant along the optimal trajectory, we have $\frac{dH}{dt} = 0$. Using $\dot{\theta} = u_1 \frac{\tan\emptyset}{d}$ and $\dot{p}_\theta = (p_x \sin\theta - p_y \cos\theta)u_1$ and $u_2 = 2p_\emptyset = \dot{\emptyset}$, it follows that:

$$\left(\dot{p}_x\cos(\theta) + \dot{p}_y\sin(\theta) + p_\theta\frac{(1 + tan(\phi)^2)}{d}p_\phi\right)u_1 - \left(\dot{p}_x\dot{x} + \dot{p}_y\dot{y}\right) = 0$$

$$-\dot{p}_\phi p_\phi = 0 \tag{28}$$

Two possibilities arise:

a) If $\dot{p}_\emptyset = 0$, then $\dot{u}_2 = 0$ which yields $u_1 = \text{const}$.
b) If $p_\emptyset = 0$, then $u_2 = 0$

In both cases, the control inputs remain constant.
Consequently, assuming that the Lagrange multiplier μ remains constant, the optimal trajectories of the system are characterized by control inputs. u_1 and u_2 that remain constant if and only if the phase of the control vector (u_1, u_2) is constant.
According to the approach described in Proposition 3, and assuming that the Lagrange multiplier μ remains constant, it has been shown that the system's optimal trajectories are characterized by constant control inputs u_1, and u_1, if and only if their phase is constant.

4.3. Hypothesis: existence of a singular arc

Following Condition 2 of Proposition 3, we propose the following hypothesis regarding the control strategy for the energy optimization problem:
Hypothesis 1. Consider a control vector U = (u_1, u_2) defined on the interval $[0, T_f]$ with corresponding control effort

$$u_1^2(t) + u_2^2(t) = C$$

Under polar parametrization, $u_1 = C_0 \cos\psi(t), u_2 = C_0 \sin\psi(t)$ with $C_0 = \sqrt{C}$ and $\psi(t)$.

We hypothesize that a singular arc exists if the control norm is constant along a segment of the trajectory, while the direction of the control, defined by

$\psi(t) = \arctan(\frac{u_2}{u_1})$,

The phase derivative satisfies the following conditions:

- If $\dot{\psi}(t) = 0$, the control direction is constant. This implies that the control is trivial and therefore not singular.
- If $\dot{\psi}(t) \neq 0$, the control direction varies with time. In this case, the control is nontrivial while maintaining a constant norm, which characterizes a singular arc.

Under this hypothesis, the vehicle applies a variable or mixed control strategy, maintaining constant total energy, and the corresponding cost functional becomes

$$J = \frac{1}{2}\int_0^{T_f} \left(u_1^2 + u_2^2\right) dt = \frac{1}{2}CT_f.$$

$$\dot{\Psi}(t) = \frac{u_1\dot{u}_2 - u_2\dot{u}_1}{u_1^2 + u_2^2} = \frac{u_1\dot{u}_2 - u_2\dot{u}_1}{C}. \quad (29)$$

This hypothesis extends the results of Condition 2 by suggesting that singular arcs correspond to segments where the total control energy is conserved, while the control direction evolves to satisfy the optimality conditions imposed by the Pontryagin Maximum Principle.

4.4. Optimal energy control without singular arc

Assuming that $\dot{\psi}(t) = 0$ (i.e., the control direction is constant, corresponding to a bang-bang strategy) and according to Equation (21), the optimal control of the truck in the presence of a circular obstacle, under the energy minimization criterion, is given by:

$$\begin{cases} u_1^* &= 2\Big(p_x \cos\theta + p_y \sin\theta + p_\theta \dfrac{\tan(\phi)}{d}\Big) \\ u_2^* &= 2p_\phi \end{cases}$$

The time derivatives of u_1^* and u_2^* are given by

$$\begin{cases} \dot{u}_1^* &= 2\Big(\dot{p}_x \cos\theta + \dot{p}_y \sin\theta + p_\theta \dfrac{1+\tan^2\phi}{d}\dot{\phi}\Big) \\ \dot{u}_2^* &= 2\Big(-\dfrac{p_\theta u_1}{d}\left(1+\tan^2(\phi)\right)\Big) \end{cases} \quad (30)$$

The condition $\dot{\psi}(t) = 0$ (cf. Equation (29)) implies that $\dot{u}_2 = 0$, with either $u_2 = 0$ or $\dot{u}_1 = 0$, since $u_1 \neq 0$.

- If $\dot{u}_2 = 0$ and $u_2 = 0$, this case is not feasible, since $u_2 \neq 0$ in the presence of an obstacle.
- If $\dot{u}_2 = 0$ and $\dot{u}_1 = 0$, in this case, according to Equation (30), and after substitution and simplification, we obtain:

$$\begin{cases} \theta = \arctan\left(\dfrac{-\dot{p}_x}{\dot{p}_y}\right) \\ \theta = \arctan\left(\dfrac{p_y}{p_x}\right) \end{cases}$$

This result leads to $\frac{p_y}{p_x} = \frac{-\dot{p}_y}{\dot{p}_x}$, which implies $\dot{p}_x p_x + \dot{p}_y p_y = 0$.
As a result, we obtain $p_x^2 + p_y^2 = 0$, and therefore $p_x = C_0\cos\theta$, $p_y = C_0\sin\theta$.
Consequently, $u_1^* = p_x\cos\theta + p_y\sin\theta = C_0(\cos^2\theta + \sin^2\theta) = C_0 = \text{const}$.
In real-world conditions, navigating a roundabout poses significant challenges for heavy or autonomous vehicles due to the dynamic behavior of surrounding traffic. Reversing or stopping maneuvers within a roundabout present serious safety risks. In this context, we assume that the vehicle's linear velocity remains positive, represented by the control constraint. $u_1 \geq 0$.
For $u_2^* = p_\emptyset = \text{const}$, the steering angle at the exit of a turn plays a crucial role. Therefore, we assume that the final condition. $\emptyset(T_f)$ is free. Otherwise, according to the transversality conditions, if $\emptyset(T_f)$ is fixed, the corresponding adjoint variable satisfies $p_\emptyset(T_f) = 0$. This would lead to $u_2^* = 0$, which is not feasible in the presence of an obstacle.
In conclusion, for a constant control phase, the optimal controls u_1^* and u_2^* for a truck-type mobile robot navigating among circular obstacles under the energy minimization criterion are constant.

5. Numerical Simulation for The Problem (EETPPPCO)

This section presents the main results of the optimal control problem (17). The simulations were performed using the direct trapezoidal collocation method, which efficiently handles trajectory constraints and high-dimensional systems [16]. Three representative scenarios are illustrated in Figure 3.

It should be noted that these results are based on simulated data rather than experimental measurements. The simulations demonstrate the effectiveness of the proposed optimal control strategy for navigating a truck-type mobile robot in environments containing circular obstacles while minimizing energy consumption. The main results include the computed optimal trajectories, control profiles, and corresponding energy consumption, highlighting the advantages of the collocation-based approach for solving complex constrained optimal control problems.

(A) Different Scenarios of A Truck Navigating A Roundabout (B) Numerical Simulation Scenarios Considered in This Study

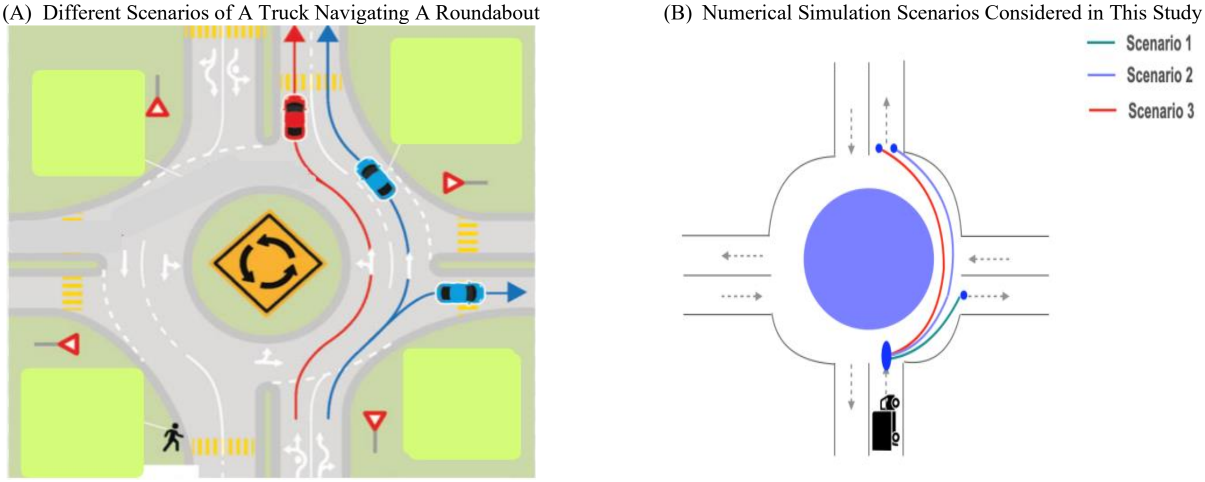

Fig. 3: Scenarios of A Truck Navigating A Roundabout.

Three representative scenarios are studied to evaluate the performance of the energy-optimal control strategy (c.f. Figure3):
1) Scenario 1: Navigation via the first exit of the roundabout.
2) Scenario 2: Navigation via the second exit with entry on the right and Exit on the right.
3) Scenario 3: Navigation via the second exit with entry on the left and exit on the left.

Scenario 1 tests the robot's ability to handle tight turns while minimizing energy consumption. Scenario 2 evaluates maneuverability with various entry and exit directions in a constrained environment. Scenario 3 explores a different entry-exit configuration to study its influence on trajectory and control effort. Together, these scenarios provide a comprehensive assessment of the proposed strategy.
The simulations were performed using the direct trapezoidal collocation method. For a system described by $\dot{X}(t) = f(X(t), U(t))$, the discretized state equations are given by:

$$\boxed{X_{k+1} = X_k + \frac{h}{2}\left[f(X_k, U_k) + f(X_{k+1}, U_{k+1})\right]} \tag{31}$$

Where $X_k = (x_k, y_k, \theta_k, \emptyset_k)$ is the state vector, N is the number of discretization points, and $h = \frac{T_f}{N}$ is the step size.
The energy cost function to be minimized is:

$$\boxed{J(U(t_k)) = \frac{1}{2}\sum_{k=0}^{N-1}\frac{h}{2}\left[(u_{1,k}^2 + u_{2,k}^2) + (u_{1,k+1}^2 + u_{2,k+1}^2)\right]} \tag{32}$$

Here, J represents a quadratic measure of control effort. While not a physical energy measurement, it provides a comparative indicator of the energy required to execute the maneuvers.
Simulation Parameters:
- Rear axle of the truck: $(x_0, y_0) = (0,0)$
- Obstacle center: $(x_{obs}, y_{obs}) = (0.5, 0.03)$, obstacle radius: robs = 1 m
- Control bounds: $u_{1,k} \in [-1, 1]$, $u_{2,k} \in [-0.35, 0.35]$
- Number of discretization points: N = 100
- Final time T_f fixed for each scenario

For consistency, the same terminal position $x(T_f) = 1$ and $y(T_f) = 0$ was imposed for Scenarios 2 and 3, enabling a direct comparison of the optimal trajectories under identical boundary conditions.

5.1. Scenario 1: navigation via the first exit of the roundabout

In Scenario 1, the robot navigates a roundabout by taking the first exit. The results are illustrated in Figure 4

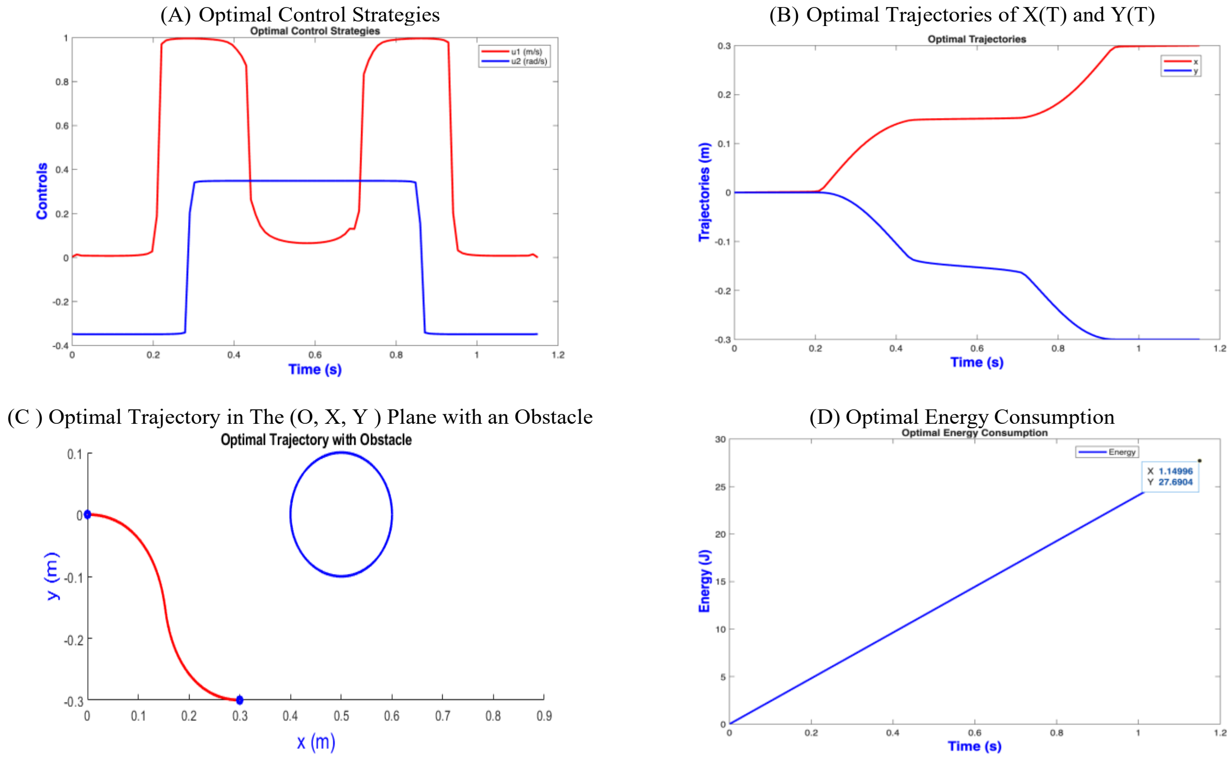

Fig. 4: Numerical Simulation Results for Scenario 1.

5.2. Scenario 2: truck navigation via the second exit of the roundabout

In Scenario 2, the robot takes the second exit and navigates the environment.

5.2.1. Case 1: entry on the right and exit on the right

This case focuses on a configuration where the robot enters and exits on the right. The numerical results are shown in Figure 5, illustrating how the robot handles the turns and maintains energy-efficient navigation.

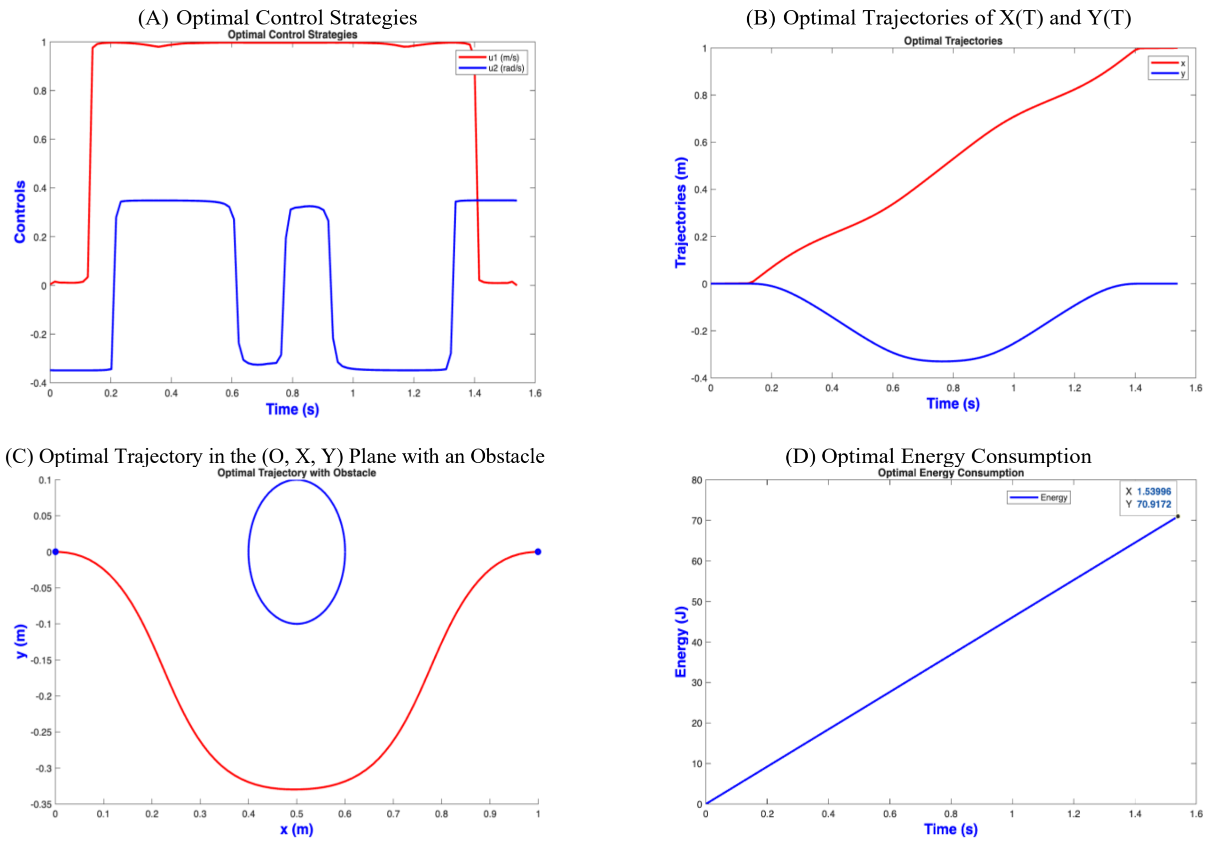

Fig. 5: Simulation Results for Scenario 2: Right-Hand Entry to Right-Hand Exit.

5.2.2. Case 2 and Case 3: right entry–right exit with a longer final time

These cases correspond to Case 2 and Case 3 and focus on a configuration in which the robot enters and exits on the right, with a longer imposed final time. The numerical results are presented in Figure 6, which illustrate how the robot performs the turns while maintaining energy-efficient navigation.

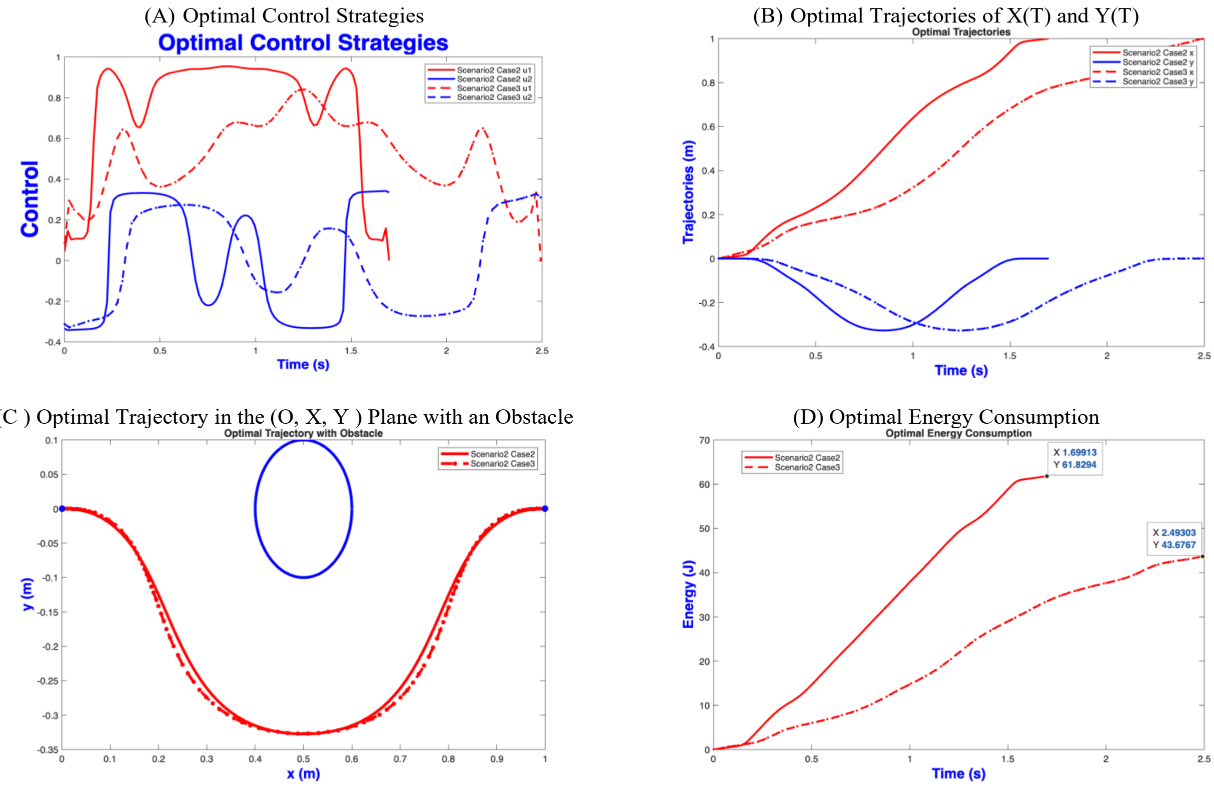

Fig. 6: Simulation Results for Scenario 2: Right Entry–Right Exit with Longer Final Time.

5.3. Scenario 3: entry on the left and exit on the left

In this case, the robot enters on the left and exits on the Left. Figure 7 shows the trajectories and control behavior, highlighting the effect of different entry/exit positions on energy consumption and maneuverability.

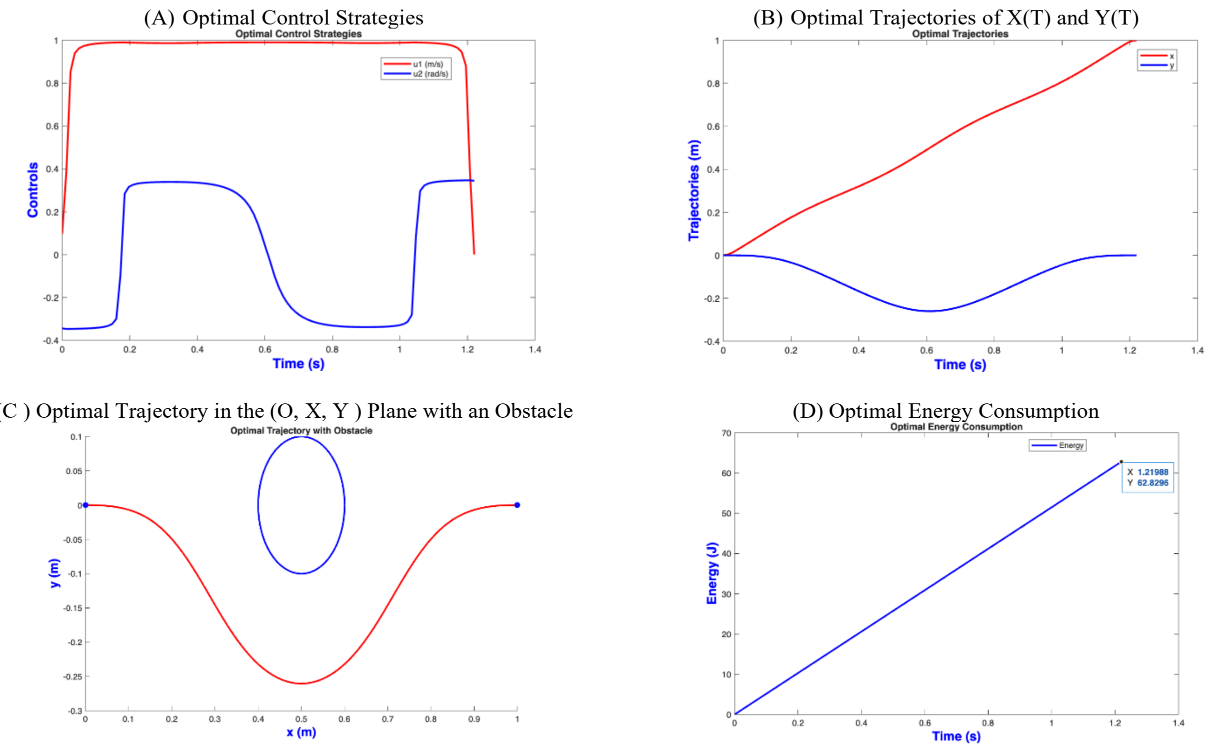

Fig. 7: Simulation Results for Scenario 3: Left-Hand Entry to Left-Hand Exit.

5.4. Comparison of scenarios based on the presence of singular arcs

A comparison of Case 1, Case 2, and Case 3 of Scenario 2 with Scenario 1 and Scenario 3 is performed under the hypothesis of the existence of a singular arc, i.e., $\dot{\psi}(t) = 0$ (cf. Hypothesis 1). Case 3 represents a scenario similar to Case 1 and Case 2 of Scenario 2, but with a longer final time. The corresponding results are illustrated in Figure 8.

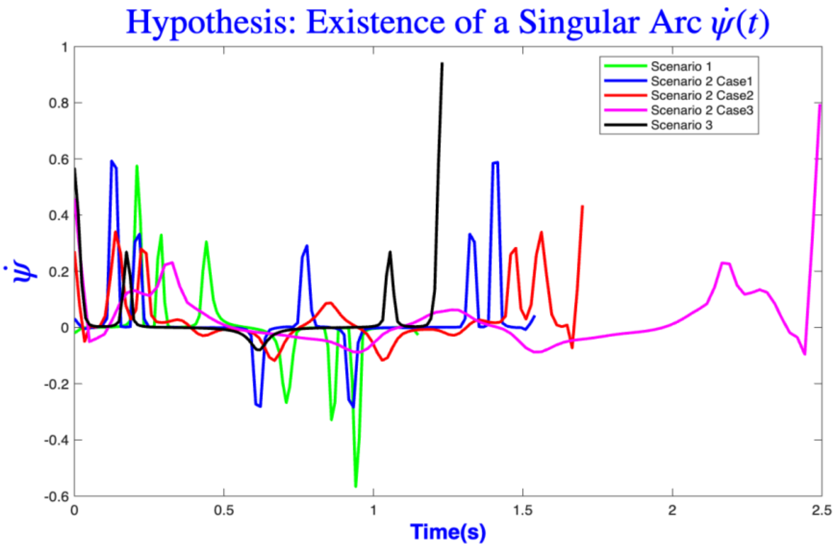

Fig 8: Numerical Comparison of Scenarios based on the Presence of Singular Arcs

5.5. Comparison of scenarios with distinct navigation configurations around the roundabout

A comparison of Case 1, Case 2, and Case 3 of Scenario 2 with Scenario 3 is presented in Figure 9. The figure highlights the differences in the optimal trajectories, emphasizing the influence of entry and exit configurations on the overall navigation performance.

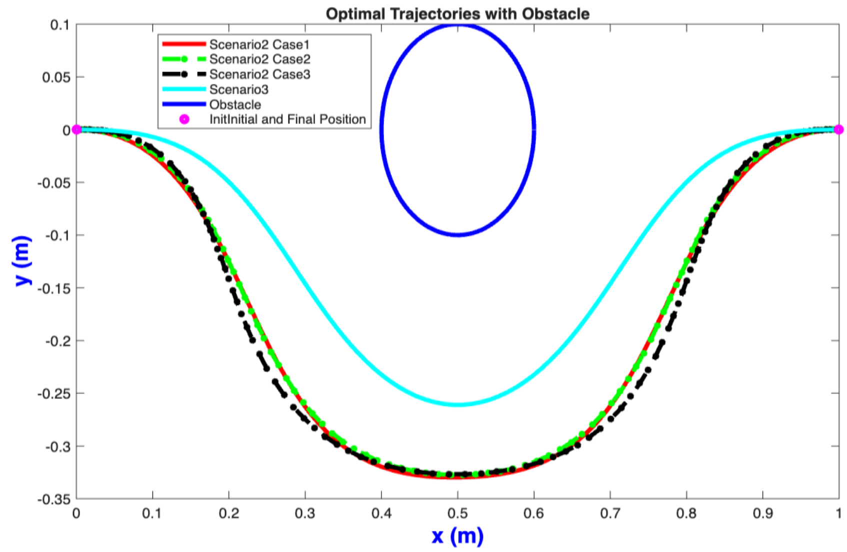

Fig. 9: Numerical Comparison of Truck Navigation between Case 1, Case 2 in Scenario 2, and Scenario 3.

5.6. Description

1) Figures 4a, 5a, 6a, and 7a show the evolution of the optimal control strategies $u_1^*(t)$ and $u_1^*(t)$, exhibiting a piecewise-constant structure. The control inputs are characterized by successive time intervals over which the controls maintain constant values (bang) or follow a singular arc, which may be either constant or variable.
2) Figures 4b, 5b, 6b, and 7b represent the optimal state trajectories. The state variables $x(t)$ and $y(t)$ evolve gradually and continuously over time. These trajectories are piecewise continuous and divided into segments, reflecting the structure of the control inputs.
3) Figures 4c, 5c, 6c, and 7c illustrate the robot's optimal paths while avoiding the circular obstacle and maintaining a prescribed safety distance. This behavior corresponds to a balanced avoidance maneuver combined with a final orientation adjustment, enabling the robot to reach the designated exit configuration.
4) Figures 4d, 5d, 6d, and 7d present the cumulative energy consumption, which evolves almost linearly over time. As shown in these figures, the total energy increases steadily and continuously, without abrupt changes or discontinuities. This regular energy evolution is a direct consequence of the structure of the control inputs.
5) Figure 8 presents numerical results illustrating the differences in the evolution of the switching function derivative $\dot{\psi}(t)$ for the considered scenarios. The objective of this comparison is to analyze the influence of singular arcs on the structure of the optimal trajectory and on the final time of the maneuver according to Hypothesis 1.

In particular, Case 3 exhibits behavior similar to Case 1 and Case 2 of Scenario 2 but with a longer final time, which directly affects the evolution of $\dot{\psi}(t)$ This comparison highlights how the presence and duration of singular arcs influence the overall trajectory, control smoothness, and total travel time.

1) Figure 9 illustrates the optimal trajectories obtained for Case 1 and Case 2 of Scenario 2 and for Scenario 3 under different navigation configurations around the roundabout. Although the same obstacle avoidance constraints are considered, the entry and exit positions differ, leading to distinct path geometries.

5.7. Discussion

- The control strategies in Scenario 1, Scenario 2 (Case 1), and Scenario 3 (cf. Figures 4a, 5a, and 7a, respectively) exhibit bang-bang behavior for both controls u_1^* and u_2^*.

In contrast, for Cases 2 and 3 of Scenario 2, the control strategies consist of a bang segment combined with singular arcs, as illustrated in Figure 6a.
According to Hypothesis 1, the performance index reduces to

$$J = \frac{1}{2} C T_f$$

Therefore, minimizing the energy becomes equivalent to minimizing the final time when the control norm remains constant.
This result is confirmed by Cases 2 and 3 of Scenario 2, as illustrated in Figure 8: an increase in the maneuver duration (final time) leads to control strategies involving longer or more pronounced singular arcs ($\dot{\psi}(t) \neq 0$). In contrast, Scenario 1, Case 1 of Scenario 2, and Scenario 3 are simulated under minimum-time and minimum-energy conditions, resulting in bang-type control strategies, i.e., $\dot{\psi}(t) = 0$, except for isolated peaks corresponding to switching instants of the controls.

- The total energy consumed, as shown in Figures 4d, 5d, 6d, and 7d, is higher in Scenario 2 (Case 1) compared to Scenarios 1 and 3. Under a bang-bang control strategy, the controls reach the limits of their admissible bounds, which leads to higher energy consumption. This behavior can be explained by the longer maneuver duration in Scenario 2 (Case 1) (final time T_f= 1.53 and energy E = 71) compared to Scenario 1 (T_f = 1.15, E = 27.7) and Scenario 3 (T_f = 1.22, E = 62.82). Since the control norm reaches its maximum value, the constant C attains its upper bound, and therefore the performance index

$$J = C T_f$$

depends primarily on the final time T_f
In the presence of a singular arc, the most efficient strategy is the one that achieves lower energy consumption while maintaining effective control performance. This observation is illustrated by Scenario 2 (Case 2) (T_f = 1.7, E = 61) compared to Scenario 2 (Case 3) (T_f = 2.5, E = 43.67). Although Case 3 has a longer final time, it consumes less energy than the purely bang-bang strategy observed in Scenario 2 (Case 1) (T_f = 1.53, E = 71). This result indicates that the constant C decreases when the control inputs do not remain at their saturation limits (i.e., when $u_1^2 + u_2^2 < C$). Consequently, in such cases, the energy cost J depends not only on the final time T_f but also on the variation of the control magnitude represented by the constant C.

- The comparison of different navigation configurations is presented in Figure 9.

In Case 1, Case 2, and Case 3 of Scenario 2, the robot approaches the roundabout with similar initial conditions but follows slightly different steering strategies, resulting in variations in curvature and maneuver duration. These differences are mainly associated with the switching structure of the control inputs and the presence of singular arcs along certain trajectory segments in Case 2 and Case 3, as shown in Figure 6a.
Scenario 3 corresponds to a different navigation configuration characterized by modified entry and exit orientations. As a result, the robot follows a trajectory with a different turning pattern around the circular obstacle, which directly affects the path length and the total travel time. The comparison highlights the sensitivity of the optimal trajectory to boundary conditions, particularly the initial and final configurations. Even small changes in the entry or exit positions can lead to noticeable differences in the trajectory shape, control sequence, and maneuver duration. Overall, this analysis demonstrates that navigation performance around the roundabout is strongly influenced by geometric constraints and configuration settings. Understanding these effects is essential for designing robust and efficient motion planning strategies in environments containing circular obstacles.

6. Comparison between Theoretical Results via PMP and Numerical Simulation

The numerical results obtained using the direct trapezoidal collocation method are in strong qualitative agreement with the structure predicted by Pontryagin's Maximum Principle (PMP). In particular, the optimal control inputs ($u_1^*(t)$,$u_2^*(t)$) computed numerically reflect the key features derived from the theoretical analysis:

- In all cases where the PMP analysis predicts a purely bang-bang structure, the numerical controls remain piecewise-constant and exhibit sharp switching events, consistent with $\dot{\psi}(t) = 0$ except at the switching instants.
- In cases where singular arcs are theoretically predicted ($\dot{\psi}(t) \neq 0$) the numerical solutions display smooth control variations over the corresponding intervals, accurately capturing the singular behavior. These smooth segments correspond to a control magnitude below the maximum bound, reflecting the energy-efficient modulation of u1 and u2 along the singular arc.
- The numerical evolution of the switching function derivative $\dot{\psi}(t)$ aligns with the PMP predictions. During bang-bang intervals, $\dot{\psi}(t) = 0$, while over singular arcs, $\dot{\psi}(t)$ deviates from zero, indicating the continuous adjustment of the control to satisfy the optimality conditions.
- The influence of the singular arcs on the performance index $J = \frac{1}{2} C T_f$ is also confirmed numerically.

Since $C = u_1^2 + u_2^2$ is reduced during singular arcs (controls do not saturate), the energy cost J becomes dependent not only on the final time T_f but also on the amplitude and duration of the singular segments. Numerical results show that scenarios with longer singular arcs tend to achieve lower energy consumption for comparable maneuver times, consistent with the theoretical predictions.

- Overall, the collocation method captures both the bang-bang and singular behaviors, and the correspondence with the PMP analysis validates the theoretical characterization of the optimal trajectories, control smoothness, and associated energy consumption.

This comparison confirms that the combination of PMP and numerical collocation provides a robust framework for analyzing energy-efficient truck navigation in the presence of circular obstacles, accurately representing both the switching structure and the influence of singular arcs on the total cost.

7. Conclusion and Perspectives

In this article, we studied an optimal control problem for a vehicle-type mobile robot navigating in a roundabout under two performance criteria: time minimization and energy minimization (control effort). The theoretical analysis focused on the characterization of optimal controls using Pontryagin's Maximum Principle (PMP), based on the structure of the switching functions. The theoretical results derived from the PMP show that the controls are of bang-bang type in the minimum-time case without obstacles and remain bang-bang in the presence of circular obstacles under certain conditions. The PMP analysis also indicates that optimal controls in the energy-minimization case are smoother and may include singular arcs, leading to more moderate control magnitudes over the maneuver duration.

For the energy-minimization problem, we investigated optimal navigation scenarios involving obstacle avoidance in the presence of circular obstacles. A numerical approach based on the direct trapezoidal collocation method was implemented to analyze the influence of the obstacle on the system trajectory in the plane, on the time evolution of the rear axle center coordinates, and on energy consumption through appropriate control strategies. The numerical results show that the robot generally uses piecewise-constant controls to achieve circular obstacle avoidance under the energy-minimization criterion. Although the direct method does not provide theoretical optimality guarantees, it produces satisfactory results that are consistent with the structure predicted by the PMP. The segmented behavior observed in the controls is mainly related to the discretization inherent to the numerical method. These results demonstrate that the direct trapezoidal collocation method provides an effective framework for computing feasible control strategies with moderate energy consumption depending on the navigation scenario.

As a research perspective, it would be valuable to consider an experimental validation of the obtained results, particularly on a mobile robotic platform or within an advanced simulation framework. Such an extension would make it possible to assess the robustness and practical relevance of the proposed strategies in contexts closer to real-world applications, such as autonomous driving or navigation in constrained urban environments. To further extend this work, several directions may be explored:

- Numerical simulations of the problem under the minimum-travel-time criterion,
- Numerical investigations highlighting the influence of wheelbase length on trajectory behavior,
- The study of optimal control problems for other vehicle models, such as tricycle or unicycle systems, under the same performance criteria,
- The introduction of disturbances or uncertainties into the dynamic model (e.g., wind or friction effects), as well as the weighting of energy-related costs,
- Explicit comparisons with other control approaches, for example, between Model Predictive Control (MPC) and the Pontryagin Maximum Principle (PMP) in practical navigation contexts,
- Develop an autonomous roundabout management strategy with an autopilot mode, accounting for truck dimensions and operational constraints.

References

[1] Joslin Numbi, Nadjet Zioui, Mohamed Tadjine, Quantum Particle Swarm Optimisation Proportional–Derivative Control for Trajectory Tracking of a Car-like Mobile Robot, February 2025. https://doi.org/10.3390/electronics14050832.

[2] Shuang Wang, Gang Li, Jialin Song, Boju Liu, Research on an Intelligent Vehicle Trajectory Tracking Method Based on Optimal Control Theory, April 2024. https://doi.org/10.3390/wevj15040160.

[3] Ma Jin, Mingcheng Qu,,Qingyang Gao, Zhuo Huang, Tonghua Su, Zhongchao Liang, Ad vanced Trajectory Planning and Control for Autonomous Vehicles with Quintic Polynomials, December 2024. https://doi.org/10.3390/s24247928.

[4] Zikai Zhang, Exploring rounD Dataset for Domain Generalization in Autonomous Vehicle Trajectory Prediction, November 2024. https://doi.org/10.20944/preprints202409.2107.v1.

[5] Guangyu Zheng, PengLi, Dongsuu Wu, An Obstacle Avoidance Trajectory Planning Methodology Based on Energy Minimization (OTPEM) for the Tilt-Wing eVTOL in the Takeoff Phase, July 2024. https://doi.org/10.3390/wevj15070300.

[6] Dongryul Kim, Hyeonjeong Kim, Kyoungseok Han, Interaction-Aware Vehicle Motion Planning with Collision Avoidance Constraints in Highway Traffic, Apr 2024.

[7] Yizhen Sun, Junyou Yang, Donghui Zhao, YuShu, ZihannZhang, Shuoyuu Wang, A Global Trajectory Planning Framework Based on Minimizing the Risk Index, June 2023.

[8] Ding Dong, Hongtao Ye,Wenguang Luo,Jiayan Wen, Dan Huang, Collision Avoidance Path Planning and Tracking Control for Autonomous Vehicles Based on Model Predictive Control, August 2024. https://doi.org/10.3390/s24165211.

[9] Yunlong Li, Gang Li, Xizheng Wang, Research on Trajectory Planning of Autonomous Vehicles in Constrained Spaces, September 2024.un-Ting Li, Chih-Keng Chen, Hongbin RRen, TimeOptimal Trajectory Planning and Tracking for Autonomous Vehicles, May 2024.Dingji Luo, Xuchao Huang, Yucan Huang, Mingda MMiao, XueshanGGao, OptimalTrajectory Planning for Wheeled Robots (OTPWR): A Globally and Dynamically Optimal Trajectory Planning Method for Wheeled Mobile Robots, September 2024. https://doi.org/10.3390/machines12100668.

[10] B. Chalaki, L. E. Beaver, Experimental validation of a real-time optimal controller for coordination of connected and automated vehicles in a multi-lane roundabout, IEEE Transactions, 2021. https://doi.org/10.1109/IV47402.2020.9304531.

[11] Mathias Bos, Bastiaan Vandewal, Wilm Decré, Jan Swevers, MPC-based Motion Planning for Autonomous Truck-Trailer Maneuvering, Feb 2023.

[12] Yingqing Chen, Christos G. Cassandras, Kaiyuan Xu, Optimal Sequencing and Motion Control in a Roundabout with Safety Guarantees, Mar 2024. https://doi.org/10.1109/CDC56724.2024.10886252.

[13] A. Babaei Robat, C. Arezoo, K. Alipour, B. Tarvirdizadeh, Dynamic modelling and trajectory tracking controller for semi-trailer-type wheeled robots, taking wheel slip into account, 2024. https://doi.org/10.1016/j.isatra.2024.03.004.

[14] J. T. Betts, Practical Methods for Optimal Control and Estimation Using Nonlinear Programming, 2nd ed., SIAM, 2010. https://doi.org/10.1137/1.9780898718577.

[15] P. Kassaeiyan, B. Tarvirdizadeh, Control of semi-trailer-type wheeled robots taking into account self-collision effect and actuator saturation limitations, 2019. https://doi.org/10.1016/j.ymssp.2019.03.016.

[16] L.E. Beaver, A long-duration autonomy approach to connected and automated vehicles, 2022.

[17] A. Bouzar Essaidi, O. Lakhal, V. Coelen, A. Belaroici, M. Haddad, R. Merzouki, Path planning for autonomous mobile robots with wheels and trailers, 2020. https://doi.org/10.1016/j.ifacol.2020.12.2657.
[18] A. Bouzar Essaidi, M. Haddad, Minimum time trajectory planning under dynamic constraints for a mobile wheeled robot with trailer, 2022. https://doi.org/10.1016/j.mechmachtheory.2021.104605.
[19] B. Chalaki, A.A. Malikopoulos, An optimal coordination framework for connected and automated vehi cles in two interconnected intersections, 2022. https://doi.org/10.1109/CDC51059.2022.9992572.
[20] H. Chitsaz, Optimal trajectories as a function of time for a car-type mobile robot with a trailer, 2013.
[21] H. Chitsaz, S. LaValle, D.J. Balkcom, M.T. Matson, Trajectory planning for mobile robots with differ ential drive, 2006.
[22] A. De Luca, G. Oriolo, C. Samson, Feedback control of a nonholonomic car-like robot, in Robot Motion Planning and Control, Springer, Berlin, Heidelberg, 2005, pp. 171–253. https://doi.org/10.1007/BFb0036073.
[23] Z. Farkas, A. Mihály, P. G., Model predictive control method for autonomous vehicles in roundabouts, 2023. https://doi.org/10.3390/machines11010075.
[24] E. Hairer, S.P. Norsett, G. Wanner, Solving Ordinary Differential Equations I: Nonstiff Problems, 1993.
[25] M. Haddad, T. Chettibi, S. Hanchi, I. Lehtihet, A random profile approach for trajectory planning of mobile wheeled robots, 2007. https://doi.org/10.1016/j.euromechsol.2006.10.001.
[26] J.P. Laumond, S. Sekhavat, M. Vaisset, Collision-free motion planning for a non-holonomic mobile robot with a trailer, 1994. https://doi.org/10.1016/S1474-6670(17)47311-3.
[27] J.P. Laumond, S. Sekhavat, F. Lamiraux, Direct lines for non-holonomic motion planning for mobile robots, 1998.
[28] K. Long, et al., Optimal controller for a roundabout with cooperative optimization, Journal of Trans portation Engineering, Part A: Systems, vol. 149, no. 1, 04022118, 2023. https://doi.org/10.1061/JTEPBS.0000780.
[29] H. Maurer, Optimal control: Theory and Numerical Methods, Lecture Notes, University of Heidelberg, 2005.
[30] C. Min, Y. Panoramique, W. Dai, I. Kawsar, Z. Li, G. Gengxiang, Optimisation of the trajectory of an electric vehicle with minimal energy consumption using an inverse dynamics model and servo constraints, 2023. https://doi.org/10.1016/j.mechmachtheory.2022.105185.
[31] O. Oukacha, N. Boizot, Consumption minimization for an academic model of a vehicle, Optimal Control Applications and Methods, vol. 41, no. 4, pp. 1288–1320, 2020. https://doi.org/10.1002/oca.2604.
[32] L.S. Pontryagin, V.G. Boltyanskii, R.V. Gamkrelidze, E.F. Mishchenko, The Mathematical Theory of Optimal Processes, Wiley, 1962.
[33] T. Rizano, D. Fontanelli, L. Palopoli, L. Pallottino, P. Salaris, Global trajectory planning for competitive robotic cars, 2013. https://doi.org/10.1109/CDC.2013.6760584
[34] K. Shojaei, Intelligent and coordinated control of an autonomous semi-trailer and a combine harvester, 2021. https://doi.org/10.1016/j.ejcon.2021.02.005
[35] O. Stryk, R. Bulirsch, Direct and indirect methods for trajectory optimisation, 1992. https://doi.org/10.1007/BF02071065.
[36] F. Tarhini, R. Talj, M. Doumiati, Safe and energy-efficient jerk-controlled speed profiling for on-road autonomous vehicles, 2022.
[37] J. Villagra, V. Milanés, J. Pérez, J. Godoy, Smooth planning of trajectories and speeds for automated public transport vehicles, 2012. https://doi.org/10.1016/j.robot.2011.11.001.
[38] R. Walambe, N. Agarwal, S. Chou, V. Joshi, Generation of optimal trajectories for a car-type mobile robot using spline interpolation, 2016.
[39] H. Wang, Y. Chen, P. Souéres, an efficient geometric algorithm for calculating optimal trajectories in real time for a car-type robot, 2007.
[40] Modeling of Mobile Robots, CHAPTER II, University of BATNA2
[41] R. Wu, H. Jia, L. Yang, H. Miao, Y. Lin, Y. Zhang, A distributed trajectory control strategy for connected automated vehicles in an isolated roundabout, 2023.
[42] K. Xu, C.G. Cassandras, W. Xiao, Decentralized time and energy-optimal control of connected and automated vehicles in a roundabout, 2018.
[43] T. Zhao, P. Li, Y. Lin Zhang, Y. Zhao, Trajectory planning and tracking control for a mobile tractor trailer robot subject to multiple constraints, 2024. https://doi.org/10.3390/act13030109
[44] L. Zhao, A. Malikopoulos, J. Rios-Torres, Optimal control of connected and automated vehicles at roundabouts: An investigation in a mixed-traffic environment, IFAC-PapersOnLine, vol. 51, no. 9, pp. 73–78, 2018. https://doi.org/10.1016/j.ifacol.2018.07.013.